# Reduced-order-quadrature model for binary neutron star merger parameter estimation

Presented by:

### Nishkal Rao

Indian Institute of Science Education and Research, Pune

Dr. Homi Bhabha Road, Pune, India

Supervised by:

### Sebastiano Bernuzzi

Theoretisch-Physikalisches Institut,

Friedrich-Schiller-Universität, Jena, Germany



Friedrich-Schiller-Universität Jena Theoretisch-Physikalisches Institut

# Certificate of Completion

This is to certify that Nishkal Rao from the Indian Institute of Science Education and Research, Pune, has successfully completed the summer research project on

Reduced-Order Quadrature Model for Binary Neutron Star Merger Parameter Estimation

under the supervision of Prof. Sebastiano Bernuzzi during the period from May 2024 to August 2024.

His project work was outstanding, and he has demonstrated a high level of academic excellence and research ability.

Theoretisch-Physikalisches Institut

Friedrich-Schiller-Universität Jeno
Max-Wien-Platz 1
D-07743 Jena
DEUTSCHLAND / GERMANY

Supervisor's Signature: Prof. Sebastiano Bernuzzi Friedrich-Schiller-Universität Jena

Smithmi

Date: October 4, 2024

# Abstract

The project focuses on the development of a Reduced-Order Quadrature (ROQ) model to significantly reduce computational costs during gravitational wave parameter estimation from binary neutron star mergers. By leveraging the TEOBResumSPA waveform model and empirical interpolation methods, the study successfully demonstrates the acceleration of Bayesian inference for the inspiral and post-merger stages of the GW170817 event. The project's outcome contributes to faster and more efficient gravitational-wave astronomy, enabling real-time analysis of complex waveforms with high precision.

# Contents

1	Intr	roduction	1
	1.1	Parameter Estimation	1
	1.2	Reduced Order Quadratures	
	1.3	Deriving and Implementing the ROQs	
	1.4	Algorithm Summary	
<b>2</b>	Demonstration with GW170817		5
	2.1	Workflow of Analysis	5
3	Combining the Inspiral and Post-Merger Likelihoods		
	3.1	Modified Likelihood function	7
	3.2	Source Code	7
4	Implementation		
	4.1	ROQ Inpsiral Basis for TEOBResumSPA_NRPMW	8
	4.2	ROQ PE with TEOBResumSPA_NRPMw	
Bibliography			

## 1. Introduction

#### 1.1 Parameter Estimation

For parameter estimation studies, we are interested in computing the posterior probability density function (PDF)

$$p(\vec{\Lambda}|d) = \frac{\mathcal{P}(\vec{\Lambda}) \ \mathcal{L}(d|\vec{\Lambda})}{\mathcal{Z}(d)},$$

on the set of model parameters  $\vec{\Lambda}$ , where  $\mathcal{P}(\vec{\Lambda})$  is the prior probability on the model parameters,  $\mathcal{L}(d|\vec{\Lambda})$  is the likelihood of the data and  $\mathcal{Z}(d)$  is known as the Bayesian evidence and describes the probability of the data given the model. The evidence is typically used for model selection and enters only as an overall scaling in parameter estimation.

Assuming the detector data d contains the GW signal  $h(\vec{\Lambda}_{\tt true})$  and noise n, the log-likelihood function can be computed as

$$\log \mathcal{L}(d|\vec{\Lambda}) = -\frac{1}{2}(d - h(\vec{\Lambda}), d - h(\vec{\Lambda})),$$

where  $d = h(\vec{\Lambda}_{true}) + n$  and (a, b) is an overlap integral:

$$(d, h(\vec{\Lambda})) = 4\Re \Delta f \sum_{k=1}^{L} \frac{\tilde{d}^*(f_k)\tilde{h}(f_k; \vec{\Lambda})}{S_n(f_k)}.$$

Here  $\tilde{d}(f_k)$  and  $\tilde{h}(f_k; \vec{\Lambda})$  are the discrete Fourier transforms at frequencies  $\{f_k\}_{k=1}^L$  and  $S_n(f_k)$  is the detector's noise power spectral density (PSD).

For a given observation time  $T = 1/\Delta f$  and detection frequency window  $(f_{\text{high}} - f_{\text{low}})$  there are  $L \sim \text{int}([f_{\text{high}} - f_{\text{low}}]T)$  sampling points in the likelihood inner product. When L is large and  $\vec{\Lambda}$  must be sampled extensively there are three bottlenecks: (i) evaluation of the model at each  $f_k$ ; (ii) numerically computing the sum in the likelihood; and (iii) repeated evaluation of the likelihood.

## 1.2 Reduced Order Quadratures

Reduced Order Modeling (ROM) [1] is a promising technique for mitigating the computational cost of gravitational-wave parameter estimation. A ROM approach seeks to find a computationally efficient representation of the waveform model. If a set of N < L basis elements can be found which accurately spans the continuum template space, it is possible to replace the overlap with a quadrature rule containing only N terms, reducing the overall cost by a factor of L/N.

We shall use a combination of the reduced basis method and the empirical interpolation method, whose favorable computational efficiency, ease-of-parallelization and numerical stability make them attractive candidates for tackling waveform systems and other challenging models. The reduced basis method constructs a basis set of N elements whose span reproduces the GW model within a specified accuracy. The empirical interpolation method then uses this model-specific basis to construct an N-point interpolant defined on the model space. Substituting the empirical interpolant representation into the likelihood yields the reduced order quadrature (ROQ) rule which ultimately provides the performance gain of L/N. By selecting a small number of waveforms basis elements and an equal number of discrete interpolation frequency points, ROQs are capable of dramatically speeding up both waveform evaluation and integrals involving them, such as the Wiener inner products entering the standard GW likelihood. This is achieved by sufficiently accurate and fast to evaluate interpolants, built on a large training dataset.

### 1.3 Deriving and Implementing the ROQs

A gravitational-wave strain signal h(t) detected by a ground-based interferometer has the form

$$h(t; \vec{\Lambda}) = F_{+}(\alpha, \delta, \psi, d_L) h_{+}(t; \phi_c, t_c, \vec{\lambda}) + F_{\times}(\alpha, \delta, \psi, d_L) h_{\times}(t; \phi_c, t_c, \vec{\lambda}),$$

where the antenna patterns  $F_{(+,\times)}$  project the gravitational wave's +- and ×-polarization states,  $h_{(+,\times)}$ , into the detector's frame.

The antenna patterns are functions of variables which specify the orientation of the detector with respect to the binary: the distance to the source  $(d_L)$  as well as the right ascension  $(\alpha)$ , declination  $(\delta)$  and polarization  $(\psi)$  angles. These four variables, along with the coalescence time  $(t_c)$  and its orbital phase at coalescence  $(\phi_c)$ , describe the signal's dependence on parameters that have a trivial effect on the waveform's amplitude and phase.

We shall use  $\vec{\lambda}$  to denote the signal's dependence on parameters that have a non-trivial effect on the waveform's amplitude and phase, such as its masses, spin magnitude and spin orientation. The strain, and consequently the likelihood, depends on the full set of parameters  $\vec{\Lambda} = \{\alpha, \delta, \psi, r, t_c, \phi_c, \vec{\lambda}\}.$ 

When discussing waveform models, it is common practice to first introduce a complex gravitational wave strain

$$h_{+}(t;\phi_{c},t_{c},\vec{\lambda}) - ih_{\times}(t;\phi_{c},t_{c},\vec{\lambda}) = \sum_{\ell=2}^{\infty} \sum_{m=-\ell}^{\ell} h^{\ell m}(t;\phi_{c},t_{c},\vec{\lambda})_{-2} Y_{\ell m},$$

which is subsequently decomposed into a basis of spin-weighted spherical harmonics. Most gravitational waveform models make predictions for the modes  $h^{\ell m}(t; \vec{\lambda})$ , from which a model of what a noise-free detector records,  $h(t; \vec{\Lambda})$ , is readily recovered.

The remainder of this subsection sketches the steps leading to the reduced order quadrature rule. To build computationally efficient approximations, we work directly with the Fourier transform of the strain

$$\begin{split} \tilde{h}(f;\vec{\Lambda}) &= \int_{-\infty}^{\infty} h(t;\vec{\Lambda}) \mathrm{e}^{2\pi \mathrm{i} f t} dt \\ &= F_{+} \tilde{h}_{+}(f;\phi_{c},t_{c},\vec{\lambda}) + F_{\times} \tilde{h}_{\times}(f;\phi_{c},t_{c},\vec{\lambda}) \\ &= \mathrm{e}^{-2\pi \mathrm{i} f t_{c}} \left[ F_{+} \tilde{h}_{+}(f;\phi_{c},0,\vec{\lambda}) + F_{\times} \tilde{h}_{\times}(f;\phi_{c},0,\vec{\lambda}) \right] \end{split}$$

where the antenna pattern's arguments are omitted for brevity. The last equality follows from  $h(t;t_c) = h(t-t_c;0)$ , as a non-zero coalescence time  $t_c$  simply offsets the signal's time-of-arrival. Because  $\tilde{h}_{(+,\times)}$  enters linearly into (d,h) and quadratically into (h,h), one of the goals of this paper is to build (temporarily focusing on the model's internal parameterization  $\vec{\lambda}$ ) an approximation

$$\tilde{h}_{\mathrm{A}}(f_i; \vec{\lambda}) \approx \sum_{j=1}^{N_{\mathrm{L}}} B_j(f_i) \tilde{h}_{\mathrm{A}}(F_j; \vec{\lambda}), \quad \text{with } \mathrm{A} \in \{+, \times\},$$

$$\Re\left[\tilde{h}_{\mathrm{A}}(f_{i};\vec{\lambda})\tilde{h}_{\mathrm{B}}^{*}(f_{i};\vec{\lambda})\right] \approx \sum_{k=1}^{N_{\mathsf{Q}}} C_{k}(f_{i}) \Re\left[\tilde{h}_{\mathrm{A}}(\mathcal{F}_{k};\vec{\lambda})\tilde{h}_{\mathrm{B}}^{*}(\mathcal{F}_{k};\vec{\lambda})\right] , \quad \text{with } \mathrm{A}, \mathrm{B} \in \{+, \times\} ,$$

that accurately approximates both the polarization states and their products. Here the labels A and B take the values  $(+, \times)$ ,  $\{B_j\}_{j=1}^{N_{\rm L}}$  is the reduced basis (RB) for the polarizations and  $\{C_k\}_{k=1}^{N_{\rm Q}}$  is the RB for the real part of all possible products of the polarizations. Notice that  $\tilde{h}_+$  and  $\tilde{h}_\times$  share the same basis  $\{B_j\}_{j=1}^{N_{\rm L}}$ . Similarly the approximation to the products  $\tilde{h}_+\tilde{h}_+^*$ ,  $\tilde{h}_\times\tilde{h}_\times^*$  and  $\Re\tilde{h}_+\tilde{h}_\times^*$  also share a basis  $\{C_k\}_{k=1}^{N_{\rm Q}}$ .

The values  $\tilde{h}_{A}(\vec{\lambda}; F_{j})$  are evaluations of the A-polarization states at the *empirical* interpolation nodes  $\{F_{j}\}_{j=1}^{N_{L}}$ . The location of these nodes are uniquely selected to yield accurate interpolation with the set of basis vectors  $\{B_{j}\}_{j=1}^{N}$ . Similarly, polarization products  $\tilde{h}_{A}(\mathcal{F}_{k}; \vec{\lambda})\tilde{h}_{B}^{*}(\mathcal{F}_{k}; \vec{\lambda})$  are evaluated at a set of empirical interpolation nodes  $\{\mathcal{F}_{k}\}_{k=1}^{N_{Q}}$ , which are distinct from  $\{F_{j}\}_{j=1}^{N_{L}}$ . The approximation is known as an *empirical* interpolant, and its substitution into the inner product yields a reduced order quadrature (ROQ) rule.

We break the likelihood into those pieces which we can approximate

$$2 \log \mathcal{L} = 2(d, h) - (h, h) - (d, d)$$

$$= 2F_{+}(d, h_{+}) + 2F_{\times}(d, h_{\times}) - |F_{+}|^{2} (h_{+}, h_{+})$$

$$- |F_{\times}|^{2} (h_{\times}, h_{\times}) - 2F_{+}F_{\times}(h_{+}, h_{\times}) - (d, d)$$

$$\approx 2F_{+}(d, h_{+})_{ROQ} + 2F_{\times}(d, h_{\times})_{ROQ} - |F_{+}|^{2} (h_{+}, h_{+})_{ROQ}$$

$$- |F_{\times}|^{2} (h_{\times}, h_{\times})_{ROQ} - 2F_{+}F_{\times}(h_{+}, h_{\times})_{ROQ} - (d, d)$$

On substituting the approximations into the inner products, we derive the linear

$$(d, h_{\mathrm{A}}(\vec{\lambda}))_{\mathrm{ROQ}} \approx \sum_{j=1}^{N_{\mathrm{L}}} \omega_{j}(t_{c}) \tilde{h}_{\mathrm{A}}(F_{j}; \vec{\lambda}),$$

$$\omega_j(t_c) = 4\Re \Delta f \sum_{i=1}^L \frac{\tilde{d}^*(f_i)B_j(f_i)}{S_n(f_i)} e^{-2\pi i t_c f_i}$$

and quadratic ROQs

$$(h_{\mathrm{A}}(\vec{\lambda}), h_{\mathrm{B}}(\vec{\lambda}))_{\mathrm{ROQ}} pprox \sum_{k=1}^{N_{\mathrm{Q}}} \psi_k \tilde{h}_{\mathrm{A}}(\mathcal{F}_k; \vec{\lambda}) \tilde{h}_{\mathrm{B}}^*(\mathcal{F}_k; \vec{\lambda}) ,$$

$$\psi_k = 4 \Re \Delta f \sum_{i=1}^L \frac{C_k(f_i)}{S_n(f_i)} ,$$

Using the definition of the weights and the reality of the basis set  $\{C_k\}_{k=1}^{N_{\mathbb{Q}}}$ , expression can be written in a convenient form for numerical implementation as

$$2\log \mathcal{L}(d|\vec{\Lambda})_{\text{ROQ}} + (d,d) = 2\Re \sum_{j=1}^{N_{\text{L}}} \omega_j(t_c) \tilde{h}(F_j;\vec{\Lambda}) - \sum_{k=1}^{N_{\text{Q}}} \psi_j \tilde{h}(\mathcal{F}_k;\vec{\Lambda}) \tilde{h}^*(\mathcal{F}_k;\vec{\Lambda}).$$

Compared to the usual likelihood expression, using the typical overlap

$$2 \log \mathcal{L}(d|\vec{\Lambda}) + (d,d) = 2\Re \sum_{l=1}^{L} \frac{4\Delta f \tilde{d}^{*}(f_{l})}{S_{n}(f_{l})} \tilde{h}(f_{l};\vec{\Lambda}) - \sum_{l=1}^{L} \frac{4\Delta f}{S_{n}(f_{l})} \tilde{h}(f_{l};\vec{\Lambda}) \tilde{h}^{*}(f_{l};\vec{\Lambda}),$$

shows the ROQ rule to be similar to the standard evaluation pattern, thereby allowing existing codes to easily implement these tools.

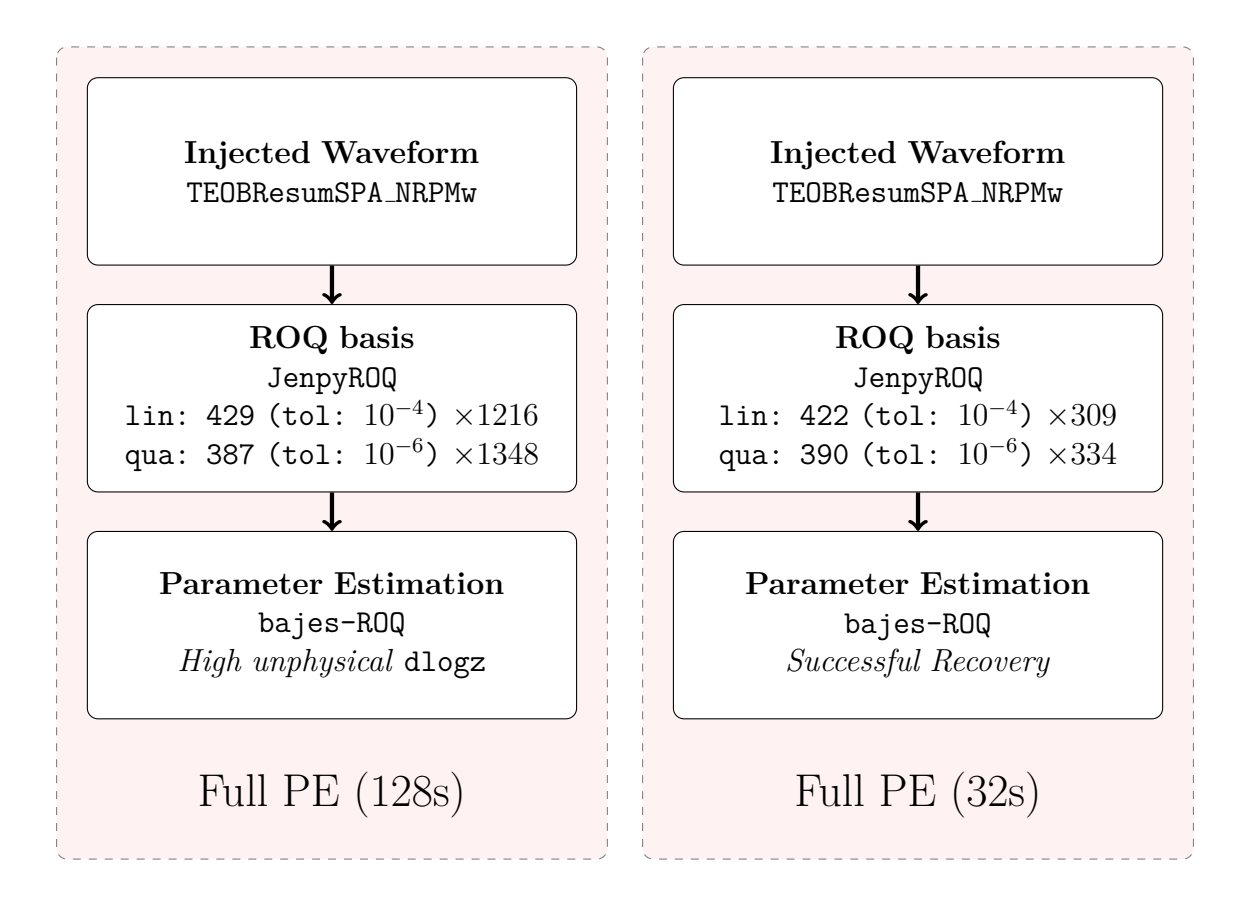
## 1.4 Algorithm Summary

We employ the JenpyROQ algorithm, presented in Tissino et al. [2], which is an updated version of the PyROQ algorithm, presented in Smith et al. [1]. In the first step of the algorithm, a pre-selected dataset of waveform vectors (typically referred to as basis) is constructed. Elements are then augmented by randomly generating a waveform dataset, and adding to the basis the element with the largest residuals after projection onto the basis. This is repeated until a user-specified tolerance is reached. In a second step, the pre-selected basis is enriched by generating increasingly larger datasets which might have different tolerance thresholds. In each of these datasets, the element with the largest interpolation error is added onto the basis, iterating until all the elements of the dataset can be represented with a given accuracy.

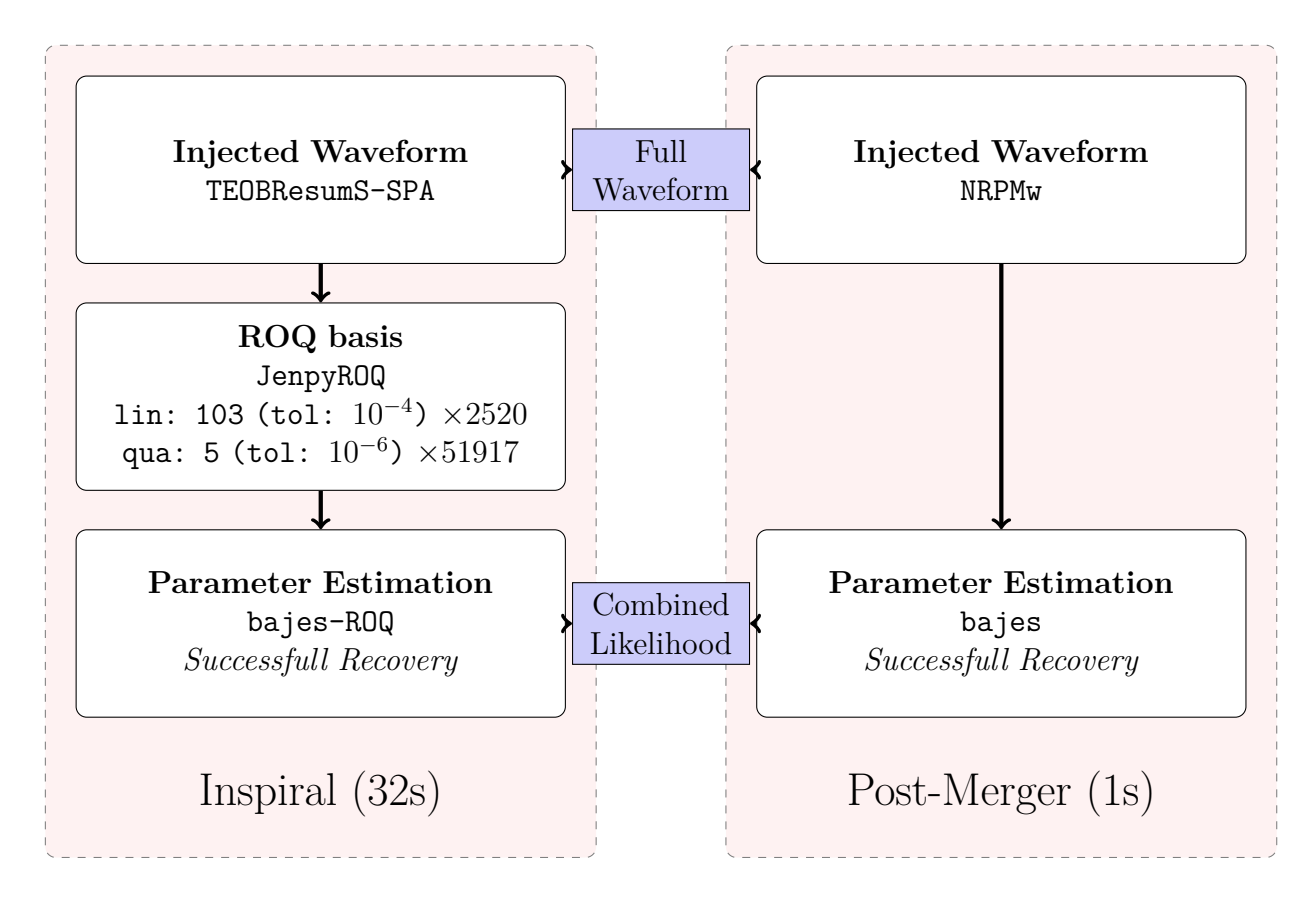
# 2. Demonstration with GW170817

## 2.1 Workflow of Analysis

Firstly, we inject the full signal consisting of the inspiral and post-merger components, and build ROQ bases for the same, to be followed by parameter estimation.



Alternatively, we compute the inspiral and post-merger components independently, and combine the likelihoods. The ROQ basis for the inspiral speeds up computation upto the frequency of merger, and then is followed by the PE likelihood of the post merger.



# 3. Combining the Inspiral and Post-Merger Likelihoods

#### 3.1 Modified Likelihood function

Since the bottleneck in the ROQ analyses results in the relentless computation of the likelihood over all frequency bins, while it exclusively speeds up in the inspiral regime, we proceed forward to compute the likelihood in parts.

Assuming the detector data d contains the GW signal  $h(\vec{\Lambda}_{\text{true}})$  and noise n, the log-likelihood function can be computed as

$$\begin{split} \log \mathcal{L}(d|\vec{\Lambda}) &= -\frac{1}{2}(d - h(\vec{\Lambda}), d - h(\vec{\Lambda})) \\ &= -\frac{1}{2}(d - h(\vec{\Lambda}), d - h(\vec{\Lambda}))_{\text{IM}} - \frac{1}{2}(d - h(\vec{\Lambda}), d - h(\vec{\Lambda}))_{\text{PM}} \\ &\approx -\frac{1}{2}(d - h(\vec{\Lambda}), d - h(\vec{\Lambda}))_{\text{ROQ}} - \frac{1}{2}(d - h(\vec{\Lambda}), d - h(\vec{\Lambda}))_{\text{PM}} \\ &= \log \mathcal{L}(d|\vec{\Lambda})_{\text{ROQ}} + \log \mathcal{L}(d|\vec{\Lambda})_{\text{PM}} \,, \end{split}$$

where  $d = h(\vec{\Lambda}_{true}) + n$  and (a, b) is an overlap integral:

$$(d, h(\vec{\Lambda})) = 4\Re \Delta f \sum_{k=1}^{L} \frac{\tilde{d}^*(f_k)\tilde{h}(f_k; \vec{\Lambda})}{S_n(f_k)}.$$

Here  $\tilde{d}(f_k)$  and  $\tilde{h}(f_k; \vec{\Lambda})$  are the discrete Fourier transforms at frequencies  $\{f_k\}_{k=1}^L$  and  $S_n(f_k)$  is the detector's noise power spectral density (PSD). Similarly, defining  $(a, b)_{\text{IM}}$  upto the merger frequency and  $(a, b)_{\text{PM}}$  from the merger frequency.

As defined earlier, we approximate the inspiral likelihood by the ROQ computation. Using the definition of the weights and the reality of the basis set  $\{C_k\}_{k=1}^{N_q}$ , the ROQ results in

$$2\log \mathcal{L}(d|\vec{\Lambda})_{\text{ROQ}} + (d,d)_{\text{IM}} = 2\Re \sum_{j=1}^{N_{\text{L}}; \text{ IM}} \omega_j(t_c)\tilde{h}(F_j; \vec{\Lambda}) - \sum_{k=1}^{N_{\text{Q}}; \text{ IM}} \psi_j \tilde{h}(\mathcal{F}_k; \vec{\Lambda})\tilde{h}^*(\mathcal{F}_k; \vec{\Lambda}).$$

Similarly

$$2 \log \mathcal{L}(d|\vec{\Lambda})_{\text{PM}} + (d,d)_{\text{PM}} = 2\Re \sum_{l=1}^{L; \text{ PM}} \frac{4\Delta f \tilde{d}^*(f_l)}{S_n(f_l)} \tilde{h}(f_l; \vec{\Lambda}) - \sum_{l=1}^{L; \text{ PM}} \frac{4\Delta f \tilde{h}^*(f_l; \vec{\Lambda})}{S_n(f_l)} \tilde{h}(f_l; \vec{\Lambda}),$$

### 3.2 Source Code

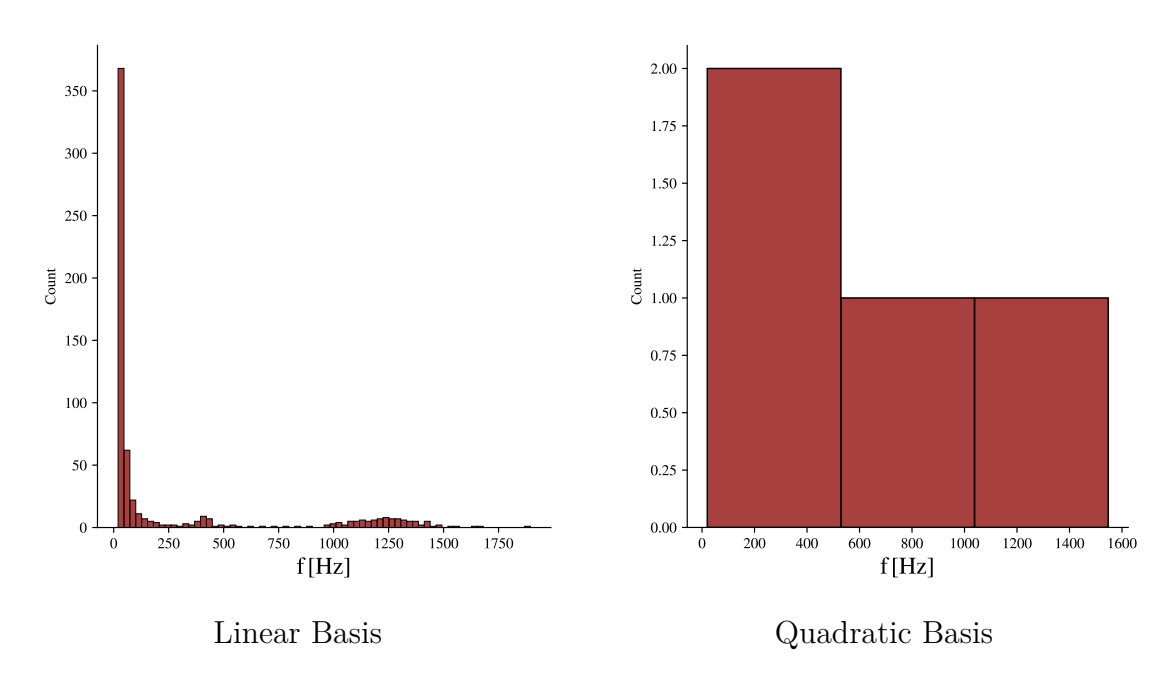
JenpyROQ is publicly available at github.com/GCArullo/JenpyROQ, TEOBResumSPA is publicly available at bitbucket.org/eobihes/teobresums/, NRPMw implemented in bajes is publicly available at github.com/matteobreschi/bajes. The Bayesian analyses presented in this work have been performed with bajes version 1.1.0, whose implementation of ROQ of the inspiral is available at github.com/nishkalrao20/bajes/tree/roq\_inspiral branch.

# 4. Implementation

### 4.1 ROQ Inpsiral Basis for TEOBResumSPA\_NRPMW

### 4.1.1 Histogram of ROQ nodes

Evidently the selected frequency points cluster at small values. This is intuitively expected because lower frequency intervals contain a greater number of waveform cycles, a feature which is automatically detected by the empirical interpolation method.

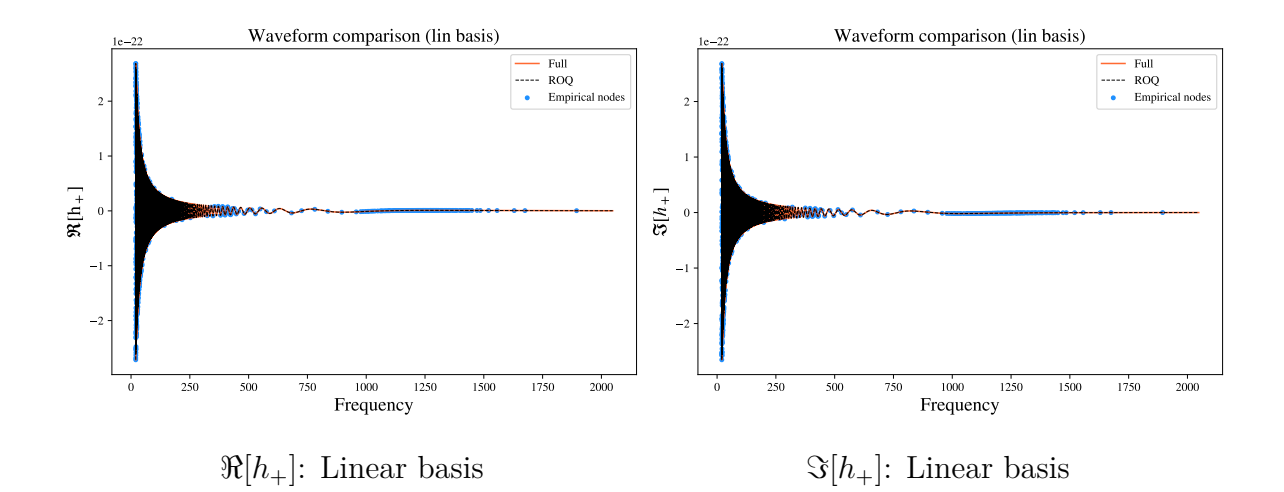


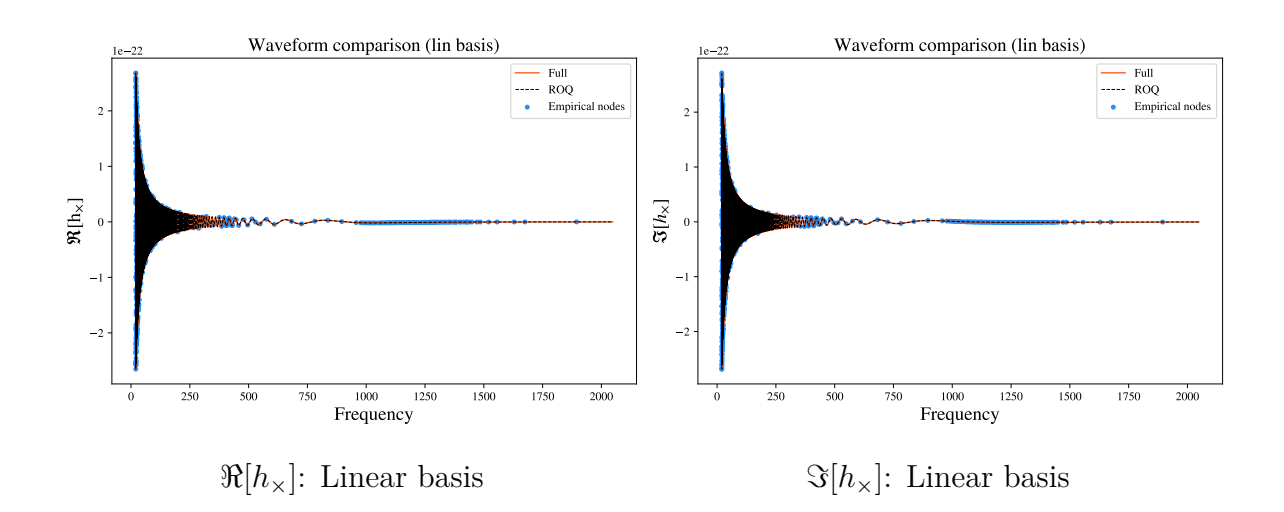
### 4.1.2 Waveform in the Linear basis

We set a tolerance threshold of  $10^{-3}$  for the linear basis, ensuring that the ROQ interpolants are valid. We use a total of  $10^3$  training datapoints, split between the pre-selection and the enrichment steps. A pre-selected basis is constructed using elements for the linear case, and  $10^3$  points at each step. We set three enrichment cycles each composed of  $10^3$  datapoints, and a respective relative tolerance of 0.1. For the PE analysis discussed above, we obtained a sufficiently accurate basis with 623 linear basis elements, achieving a linear frequency axis reduction factor of 416 times, from 259585 original frequency bins. We confirm the accuracy of the constructed interpolants by applying them to the reconstruction of validation datapoints.

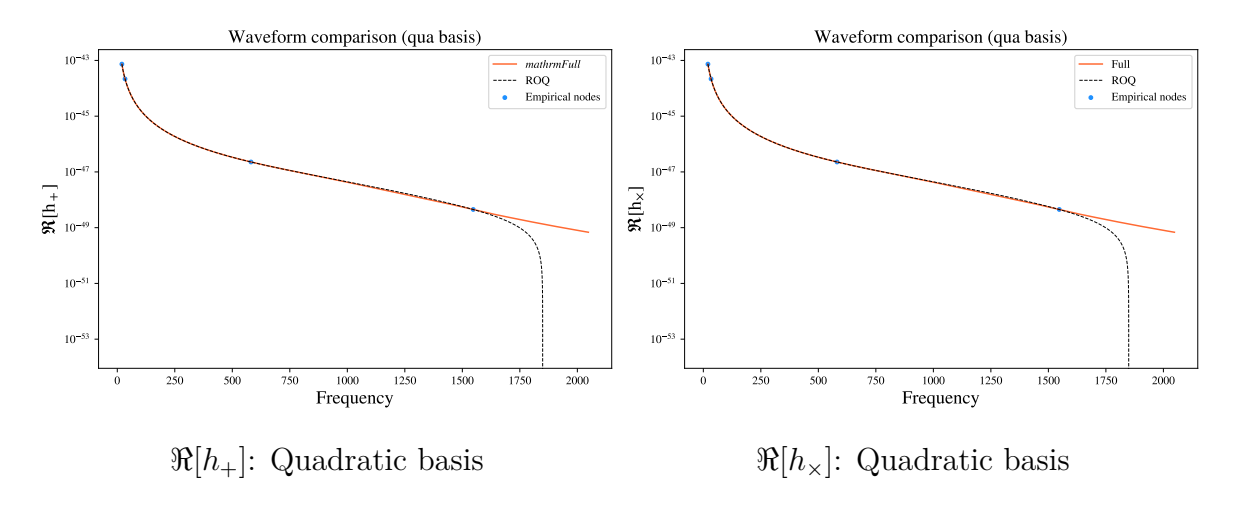
#### 4.1.3 Waveform in the Quadratic basis

We set a tolerance threshold of  $10^{-5}$  for the quadratic basis, ensuring that the ROQ interpolants are valid. We use a total of  $10^3$  training datapoints, split between the preselection and the enrichment steps. A pre-selected basis is constructed using elements for the quadratic case, and  $10^3$  points at each step. We set three enrichment cycles each composed of  $10^3$  datapoints, and a respective relative tolerance of 0.1. For the PE analysis discussed above, we obtained a sufficiently accurate basis with 4 quadratic





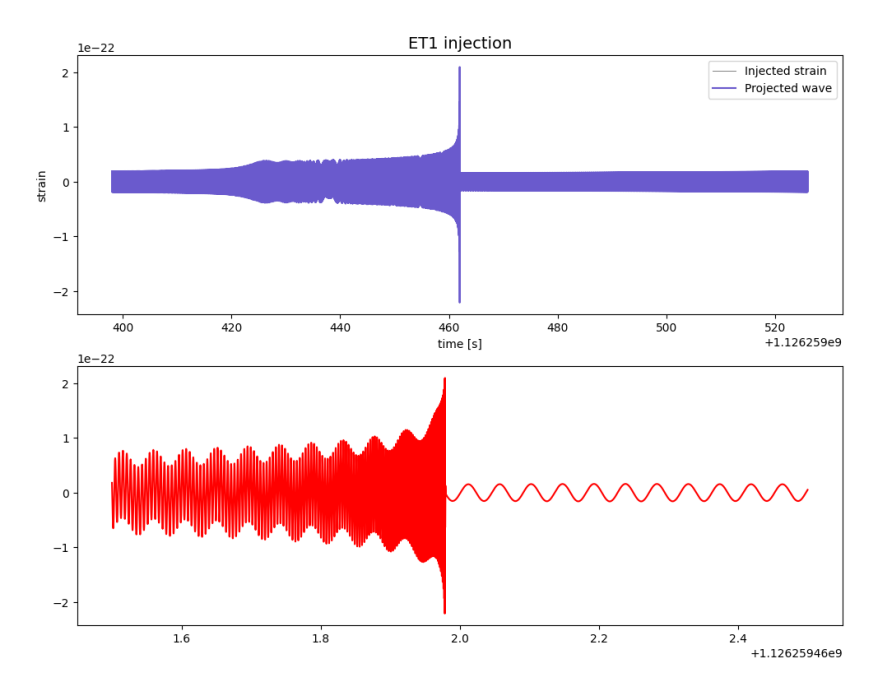
basis elements, achieving a quadratic frequency axis reduction factor of 64896 times, from 259585 original frequency bins. We confirm the accuracy of the constructed interpolants by applying them to the reconstruction of validation datapoints.



### 4.2 ROQ PE with TEOBResumSPA\_NRPMw

#### 4.2.1 Injection and Priors

We analyse an injected GW170817 like signal centered around GPS time 1126259462 with a sampling rate of 8192 Hz and a duration of 128 s, considering the frequency range from [20, 8192] Hz. Our PE relies on the MPI-parallelized bajes pipeline with ROQ inspiral support upto merger frequency of 2048 Hz encoded and the dynesty nested sampler. To summarise, the injection parameters include  $\mathcal{M}=1.188,\ q=1.,\ \Lambda_1=600,\ \Lambda_2=600,\ \iota=0.0,\ \phi_{\rm ref}=0.0,\ D_L=68{\rm MPc},\ t_{\rm coll}=14\,{\rm ms},\ \alpha=0.021,\ \phi_{\rm pm}=1.57.$ 



The mass prior is chosen to be flat in the mass components  $m_{1,2}$ , although the sampling is then performed in  $(\mathcal{M}, q)$ , with ranges wide enough to capture the full posterior width. We sample on aligned-spin components, with an isotropic prior bounded

by  $\chi_{1,2} \leq 0.8$ . The prior on the tidal parameters is uniform in the ranges  $\Lambda_{1,2} \in [5,5000]$  and the luminosity distance employs a volumetric prior. Other priors are set according to standard prescriptions in GW astronomy. We do not assume prior knowledge on electromagnetic counterparts.

# Bibliography

- [1] Rory Smith, Scott E Field, Kent Blackburn, Carl-Johan Haster, Michael Pürrer, Vivien Raymond, and Patricia Schmidt. Fast and accurate inference on gravitational waves from precessing compact binaries. *Physical Review D*, 94(4):044031, 2016.
- [2] Jacopo Tissino, Gregorio Carullo, Matteo Breschi, Rossella Gamba, Stefano Schmidt, and Sebastiano Bernuzzi. Combining effective-one-body accuracy and reduced-order-quadrature speed for binary neutron star merger parameter estimation with machine learning. *Physical Review D*, 107(8):084037, 2023.